

Photochemistry of Azoisopropane¹

Laurence D. Fogel and Colin Steel*²

Contribution from the Department of Chemistry, Brandeis University, Waltham, Massachusetts 02154. Received September 22, 1975

Abstract: The photochemistry of *cis*- and *trans*-azoisopropane (AIP) was investigated in the gas phase for direct irradiation in the wavelength range 303–366 nm ($n \rightarrow \pi^*$) and at 366 nm in solution. The pressure dependence of the quantum yields for decomposition, isomerization, and return to starting materials of both isomers indicate that AIP isomerizes via a common state, followed by rapid relaxation to vibrationally excited *cis* and *trans* ground states $C(S_0^v)$ and $T(S_0^v)$ with almost equal probability. Molecules so formed either decompose or are collisionally deactivated, the longer lived $T(S_0^v)$ being intercepted at lower pressures than $C(S_0^v)$. Evidence for the decomposition from these states is the variation in the quantum yields with wavelength and pressure, curvature in the Stern–Volmer plots for decomposition over extended pressure ranges, increased decomposition yields at elevated temperatures, and that the same photochemistry is obtained on the irradiation of both isomers when allowance is made for the difference in their heats of formation. Moreover, the lifetimes of the two dissociative states as functions of excitation energy, calculated by RRKM theory, where the Arrhenius parameters for the thermal decomposition of the isomers were employed, agree well with those determined from the quantum yield data. The data show that isomerization on direct photolysis does not proceed via the triplet manifold.

Introduction

Although acyclic azoalkane photochemistry has been the subject of considerable investigation,^{3–5} the detailed mechanism of the primary processes is not clearly understood. The main reason for this is the absence of fluorescence and phosphorescence,^{6–11} which means that the excited states cannot be monitored directly. Chemical analysis is thus the main investigative tool. It should be mentioned that with the exception of hexafluoroazomethane,¹² it is the *trans* isomer of simple azoalkanes that are commonly prepared.^{13,14} Previous gas-phase studies have in fact, therefore, been concerned with the photolysis of *trans* isomers, although this is generally not specifically stated.

In a preliminary communication,¹⁵ the intimate connection between the photochemistries of *cis*- and *trans*-azoisopropane (AIP) was discussed. It was also pointed out that the solution phase could be regarded as the limiting situation of the gas phase photochemistry at high pressures. In this paper, detailed studies of the photochemistries of both isomers in both phases and the information these data yield about the nature of the states involved in the isomerization and dissociation are reported. AIP was chosen because it is the only known aliphatic azo compound for which the *cis* isomer is thermally stable¹⁶ and whose photochemistry shows well-defined pressure dependences in easily accessible ranges. Furthermore, it was obvious from subsequent work¹⁷ that there were inconsistencies in the mechanism for photodecomposition originally proposed. In particular, the data indicated that more than one state must be involved in the photodissociation.

Experimental Section

Materials. *trans*-AIP was synthesized according to the method of Renaud and Leitch¹³ and purified by preparative GC on a 15 ft \times 1/4 in. column of 9% SF-96 on non-acid-washed Chromosorb W maintained at 80°. *cis*-AIP was prepared by the naphthalene (2.5×10^{-3} M) sensitized photoisomerization¹⁵ of the *trans* isomer (0.25 M) in cyclopentane, using Sylvania G8T5 germicidal lamps (major output at 253.7 nm) in a Rayonet photochemical reactor. After distilling off the solvent, *cis*-AIP was also purified on the above column. In the gas phase, the absorption maxima of *trans*- and *cis*-AIP were at 355 (ϵ 9.4 M⁻¹ cm⁻¹) and 380 nm (ϵ 70.2 M⁻¹ cm⁻¹), respectively. In comparison, in isoctane the maxima are at 358 (ϵ 14.8) and 380 nm (ϵ 140.2). Spectrograde isoctane was distilled and the center cut employed; the other spectroquality solvents were used without further purification. Acetophenone was vacuum distilled and the middle fraction used. Carbon dioxide was passed over a 6 ft \times 1/4 in. column

of 13X molecular sieve (30/60 mesh) to remove hydrocarbon impurities and degassed before use.

Gas-phase samples were prepared on a mercury-free, greaseless vacuum line which had been evacuated to pressures of $\leq 10^{-6}$ Torr. Gas pressures from 0 to 500 Torr were measured on a Texas Instrument quartz spiral monometer; higher pressures were read on a calibrated Matheson metal Bourdon spiral. The gas-phase photolysis vessels, a 160-cm³, 17-cm pathlength cylindrical quartz optical cell and a 500-cm³ spherical Pyrex vessel, both fitted with bellows high-vacuum valves, were conditioned by carrying out several photolyses. Mixtures of AIP and added gas were prepared by allowing the degassed AIP to equilibrate at the desired pressure in the cell and then rapidly expanding a higher pressure of added gas into the vessel. Both the sample to be photolyzed and a zero time control were prepared. The solution-phase samples were either degassed or helium flushed in 1-cm rectangular quartz cells before use.

Photolysis Apparatus and Actinometry. Since the (n, π^*) absorption band of AIP extends from 300 to 400 nm, initial samples were photolyzed in the Rayonet equipped with Sylvania F8T5/BLB black-light lamps (BLB), which had a continuous emission in the range 300–440 nm, with a maximum at 352 nm. The effective irradiation wavelengths of the isomers were determined using the absolute lamp output spectrum and the appropriate absorption spectrum. Later studies employed a 200-W high-pressure mercury lamp in conjunction with a Bausch and Lomb 500-mm grating monochromator. The intensity of the incident beam, I_0 (einstein s⁻¹), was monitored with a calibrated RCA 935 photodiode whose absolute sensitivity at 366 nm had been determined by potassium ferrioxalate actinometry^{18,19} and whose relative wavelength sensitivity was measured using a thermopile. The intensity of the transmitted beam was monitored during photolysis in order to correct for fluctuations in the lamp. The number of einsteins absorbed, I_a , was calculated from $I_a = I_0(1 - 10^{-A})t$, where A is the absorbance at the irradiation wavelength and is computed from the average of the AIP concentrations before and after photolysis, and t refers to the period of irradiation (s). Unless otherwise stated, the samples were photolyzed at 25 ± 2 °C to 2–4% (see below) to prevent significant decomposition and isomerization of the *cis* isomer formed by irradiating *trans*-AIP.

Gas-Phase Quantum Yields. The amount of AIP that decomposed or isomerized was determined by flame ionization VPC on a 9 ft \times 1/8 in. column of 3 ft of 10% SF-96 followed by 6 ft of 10% Ucon Polar, both on non-acid-washed Chromosorb W (60/80 mesh) and maintained at 80°. Decomposition quantum yields ($\Phi_{t \rightarrow d}$ and $\Phi_{c \rightarrow d}$) were measured in terms of the C₃ and C₆ hydrocarbons formed, $2C_3H_7 \rightarrow C_3H_8 + C_3H_6 + 2C_3H_7 \rightarrow C_6H_{14}$. Thus, $\Phi_{t \rightarrow d} = (\frac{1}{2}[C_3] + [C_6])/I_{a,T}$ and the quantum yield of isomerization, $\Phi_{t \rightarrow c} = [cis-AIP]/I_{a,T}$; similar equations hold when starting with *cis*-AIP. $I_{a,T}$ and $I_{a,C}$ were determined as described above. $\Phi_{t \rightarrow d}$ and $\Phi_{c \rightarrow d}$ in the absence of added CO₂ were determined absolutely by arranging the optical train so that the photodiode detected the entire light beam. These samples were then employed as relative actinometers when

samples containing CO₂ were irradiated. Since it was found that mass balance was maintained when starting with either *cis*- or *trans*-AIP, i.e., $[cis\text{-AIP}]_0$ or $[trans\text{-AIP}]_0 = [C_6]_t + \frac{1}{2}[C_3] + [trans\text{-AIP}]_t + [cis\text{-AIP}]_t$, $\Phi_{t \rightarrow c} + \Phi_{t \rightarrow i} + \Phi_{t \rightarrow d} = \Phi_{c \rightarrow c} + \Phi_{c \rightarrow i} + \Phi_{c \rightarrow d} = 1.0$. Thus, $\Phi_{c \rightarrow c}$ and $\Phi_{t \rightarrow i}$, the quantum yields for the return to starting materials, could be calculated from the experimentally determined yields.

The *trans*-AIP quantum yields were corrected for the photochemical decomposition and isomerization of the *cis* isomer formed on irradiation. It can be shown²⁰ that

$$\Phi_{t \rightarrow c}^{\text{true}} = \Phi_{t \rightarrow c}^{\text{exptl}} + (\Phi_{c \rightarrow i} + \Phi_{c \rightarrow d}) \frac{\epsilon_C [C]_{\text{av}}}{\epsilon_T [T]_{\text{av}}}$$

where $[C]_{\text{av}}$ and $[T]_{\text{av}}$ refer to the average *cis*- and *trans*-AIP concentrations and were determined by an iterative procedure, beginning with the experimentally observed concentrations. ϵ_C and ϵ_T are the extinction coefficients at the irradiation wavelength of *cis*- and *trans*-AIP, respectively; $\Phi_{c \rightarrow i}$ and $\Phi_{c \rightarrow d}$ were obtained from *cis*-AIP photolysis at the same irradiation wavelength. Similar equations can be written to correct the experimental $\Phi_{t \rightarrow d}$. The corrections were found to be significant only at the longest irradiation wavelengths where ϵ_C/ϵ_T becomes large and at high pressures of added CO₂ where isomerization is significant. For example, on BLB photolysis at room temperature with 1250 Torr of CO₂ as added gas, $\Phi_{t \rightarrow c}^{\text{exptl}} = 0.282$ while $\Phi_{t \rightarrow c}^{\text{true}} = 0.306$ and $\Phi_{t \rightarrow d}^{\text{exptl}} = 0.172$ while $\Phi_{t \rightarrow d}^{\text{true}} = 0.165$. The quantum yields reported in the figures and tables refer to these corrected values. On *cis*-isomer photolysis, the corrections were found to be negligible, since ϵ_T/ϵ_C was very small.

In addition, the quantum yields for the elevated-temperature photolysis of *trans*-AIP were corrected for the thermal decomposition of the photochemically-formed *cis*-AIP by pyrolyzing samples that had been initially photolyzed at room temperature and monitoring changes in the *cis*-AIP concentration by VPC. As expected,²¹ dark controls indicated that no *trans*-AIP thermolysis occurred at these temperatures.

Solution Quantum Yields. $\Phi_{t \rightarrow c}$ and $\Phi_{c \rightarrow i}$ were determined using Fischer-Malkin equations²² modified to allow for the decomposition that occurred in hydrocarbon solvents. The concentration of *trans*-AIP as a function of time is given by

$$[T]_t = [T]_0 - I_0(\Phi_{t \rightarrow c} + \Phi_{t \rightarrow d})\epsilon_T l \int_0^t \frac{1 - 10^{-A_t}}{A_t} [T]_t dt + I_0\Phi_{c \rightarrow i}\epsilon_C l \int_0^t \frac{1 - 10^{-A_t}}{A_t} [C]_t dt$$

where A_t is the sample absorbance at time t in a cell of pathlength l . A similar equation holds for $[C]_t$, the *cis*-AIP concentration at time t . $[C]_t$ and $[T]_t$ were determined by two methods: (1) direct VPC analysis using a 25 ft \times $\frac{1}{8}$ in. 10% SF-96 column and (2) spectral analysis. Since the absorption spectra of the isomers were known, by solving the set of equations $A_t/l = \epsilon_C[C]_t + \epsilon_T[T]_t$ at a variety of wavelengths, best values of $[C]_t$ and $[T]_t$ could be computed. Thus, A_t , $[T]_t$, $[C]_t$, and I_0 could be determined, and since $\Phi_{t \rightarrow d}$ (and $\Phi_{c \rightarrow d}$) were obtained by the same methods employed in the gas phase, $\Phi_{t \rightarrow c}$ and $\Phi_{c \rightarrow i}$ could be calculated. In addition, when a stationary state was reached in the absence of decomposition (e.g., in water), $\Phi_{t \rightarrow c}\epsilon_T[T]_{\text{ss}} = \Phi_{c \rightarrow i}\epsilon_C[C]_{\text{ss}}$; this provided another method for the determination of $\Phi_{t \rightarrow c}$ and $\Phi_{c \rightarrow i}$.

Sensitized Quantum Yields. The concentrations of the sensitizers and the azoalkanes were chosen to ensure that the former was the dominant absorber and that the latter was sufficient to efficiently intercept the donor triplet molecules. This ensured that the corrections for direct photolysis were quite small. For example, in the quenching of triplet benzophenone by *cis*-AIP in acetonitrile, the concentrations were 5×10^{-2} and 7×10^{-3} M, respectively, so that the ratio of absorbances at 303 nm was ~ 450 . The lifetime of triplet benzophenone in acetonitrile was $\sim 10^{-4}$ s,²³ while the quenching constant for *cis*-AIP was 4.9×10^9 M⁻¹ s⁻¹.²⁴ This meant that the fraction of triplets quenched was 1.0.

Degassed solutions were irradiated at 303 and 250 nm. After photolysis, the amount of isomerization that occurred was determined by spectral analysis. For AIP, decomposition and isomerization were also monitored by VPC (mixed column). The number of einsteins absorbed was calculated as described above and also by carrying out experiments in which 2,3-diazabicyclo[2.2.1]hept-2-ene (DBH) was employed as the triplet quencher, since this compound is known to decompose on sensitization with a quantum yield of unity.¹¹ In the

Table I. Quantum Yields of Azoisopropane Photoreactions in the Gas Phase

1. <i>trans</i> -Azoisopropane ^a						
λ_{irr} , nm	CO ₂ pressure,		$\Phi_{t \rightarrow d}$	$\Phi_{t \rightarrow c}$	$\Phi_{t \rightarrow i}$	
	Torr					
334.2	0		1.0	0	0	
	42		0.69	0	0.31	
	161		0.56	0.024	0.42	
	301		0.47	0.044	0.49	
	426		0.38	0.055	0.57	
	786		0.33	0.090	0.58	
	1030		0.25	0.13	0.62	
312.9	1240		0.31	0.13	0.51	
	1470		0.29	0.15	0.56	
	0		1.0	0	0	
	37		0.83	0	0.17	
	88		0.72	0	0.28	
	180		0.63	0	0.37	
	352		0.56	0	0.44	
334.2	560		0.50	0.038	0.46	
	760		0.51	0.046	0.44	
	2. <i>cis</i> -Azoisopropane ^a					
	λ , nm	CO ₂ pressure,		$\Phi_{c \rightarrow d}$	$\Phi_{c \rightarrow i}$	$\Phi_{c \rightarrow c}$
		Torr				
	365.5	0		1.0	0	0
		11		0.90	0.13	0
27			0.73	0.26	0.012	
38			0.65	0.31	0.041	
50			0.61	0.37	0.017	
87			0.52	0.41	0.069	
139			0.46	0.44	0.10	
151			0.44	0.44	0.12	
225			0.40	0.47	0.13	
251			0.41	0.49	0.099	
334.2	0		1.0	0	0	
	23		0.92	0.10	0	
	47		0.83	0.18	0	
	69		0.79	0.23	0	
334.2	102		0.72	0.30	0	
	143		0.65	0.33	0.019	
	178		0.58	0.38	0.041	
	219		0.57	0.42	0.047	

^a AIP pressure 0.25 ± 0.02 Torr, temp 25 ± 2 °C.

gas phase, the 17-cm path length quartz cell was filled with ~ 0.1 Torr of azoalkane and the appropriate amount of sensitizer was frozen into the cell. The pressure of azoalkane was always less than that of the sensitizer, so that several deactivating collisions removing any excess donor vibrational energy would occur prior to energy transfer to the azo molecule. After photolysis, the samples were analyzed by VPC (mixed column) and the quantum yields determined using gaseous DBH as the triplet counter.

Results and Discussion

Pressure Dependence of Quantum Yields for Direct Photolysis. The quantum yields of *cis*- and *trans*-AIP decomposition ($\Phi_{c \rightarrow d}$ and $\Phi_{t \rightarrow d}$), isomerization ($\Phi_{c \rightarrow i}$ and $\Phi_{t \rightarrow c}$), and return to starting material ($\Phi_{c \rightarrow c}$ and $\Phi_{t \rightarrow i}$) were determined when the AIP pressure was maintained at 0.25 ± 0.02 Torr and the pressure of carbon dioxide, the added "inert" gas, was varied from 0 to 1200 Torr. The *trans* isomer was photolyzed at 365.5, 334.2, 312.9, and 302.4 nm and the *cis* isomer at 365.5 and 334.2 nm. In addition, both compounds were photolyzed using black-light irradiation, where the effective wavelengths were 367.5 and 355 nm for *cis*- and *trans*-AIP, respectively. The data for the latter irradiations are given in Figures 1 and 2, while the effect of wavelength on *trans*-AIP photoreactions is shown in Figure 3. The remaining quantum yields are listed in Table I.

The disproportionation-to-recombination ratio of the isopropyl radicals (i.e., $[C_3H_6]/[C_6H_{14}]$ or $[C_3H_8]/[C_6H_{14}]$) could also be determined, since the decomposition quantum yields were measured in terms of these hydrocarbons rather

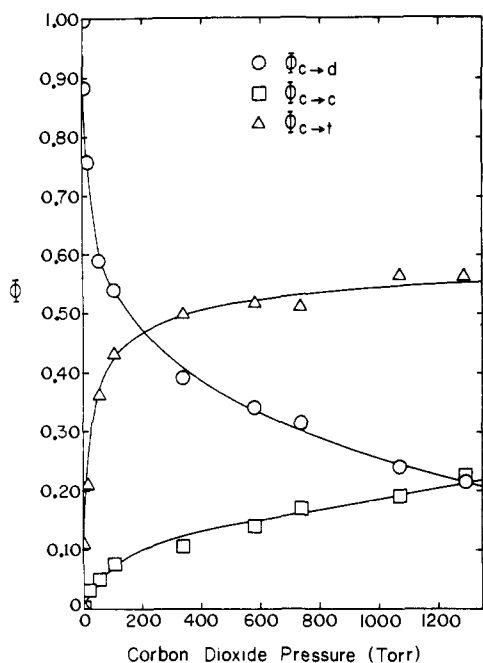


Figure 1. Pressure dependence of *cis*-azoisopropane quantum yields as a function of added gas (carbon dioxide) pressure: *cis*-AIP pressure 0.25 ± 0.02 Torr; effective wavelength of irradiation 367.5 nm.

than simply the nitrogen formation. The ratio was found to be 0.64 ± 0.02 for both isomers at all wavelengths on room-temperature photolysis, in good agreement with previously reported values for *trans*-AIP.^{25,26} Moreover, because $[C_3H_8] = [C_3H_6]$, it can be concluded that hydrogen abstraction from AIP by isopropyl radicals^{7,27} was unimportant under the experimental conditions employed. Also the identity of $[C_3H_6]/[C_6H_{14}]$ for both isomers indicates the absence of any significant amount of direct molecular C_6H_{14} formation in the photolysis of the *cis* isomer.²⁸

Direct Photolyses in Solution. Solution can be regarded as the limit of the high-pressure studies. Isomerization is now the major channel. The quantum yields obtained on direct photolysis both in a hydrogen-bonding polar solvent (water) and in a non-polar solvent (isooctane) are given in Table II. Since mass balance was also maintained in solution, $\Phi_{c \rightarrow c}$ and $\Phi_{t \rightarrow t}$ can be calculated from the data in the table. The quantum yields agree well with those previously for AIP,^{15,29} as well as with those for other acyclic azoalkanes.³ In addition, the $[C_3H_8]/[C_3H_6]$ ratio increased from 1.0 in the gas phase to 1.21 ± 0.02 in isooctane as a result of hydrogen abstraction from the solvent. Similar results have been found for the $[C_2H_4]/[C_2H_6]$ ratio in the photolysis of *trans*-azoethane.³⁰

It was also found that there was little, if any, effect of temperature or solution degassing on the rate of isomerization. Ethanolic solutions of both *cis*- and *trans*-AIP were photolyzed at 365.5 nm in the range 25 to -196° , and no changes could be detected in the rates of photoisomerization. Indeed, in the case of *trans*-azomethane (*trans*-AM), the *cis* isomer has been prepared by irradiation of the *trans* at liquid nitrogen temperature.³¹ The isomerization of several bulky azo compounds has also been observed to continue at -196° .^{3,32}

Mechanism for Direct Photolysis. In this section, a model is presented to explain the above results. Later, this mechanism shall be compared with others that have been proposed in view of the above findings and of data yet to be presented. The most obvious features to be explained are as follows. (1) In the gas phase, as pressure increases, decomposition decreases, while isomerization and return to starting materials become increasingly important. Moreover, the buildup of *trans*-AIP

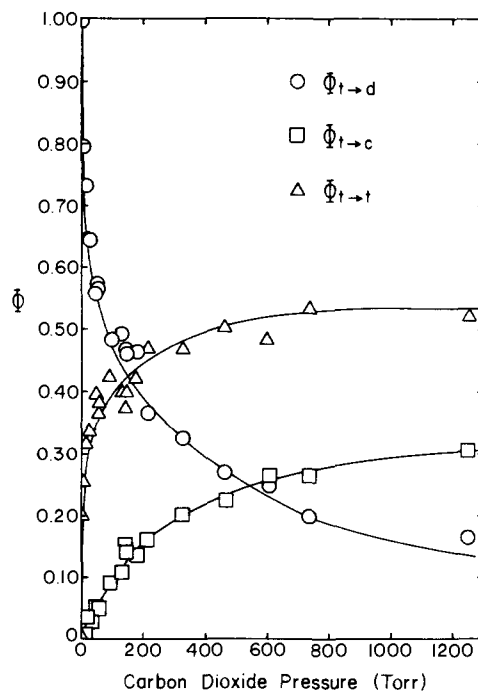


Figure 2. Pressure dependence of *trans*-azoisopropane quantum yields as a function of added gas (carbon dioxide) pressure: *trans*-AIP pressure 0.25 ± 0.02 Torr; effective wavelength of irradiation 355 nm.

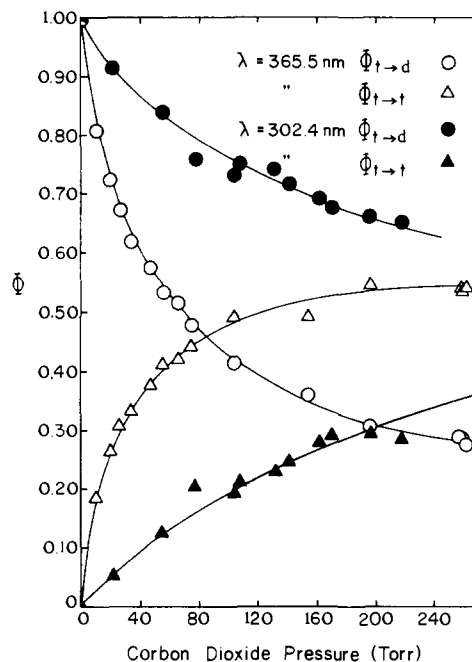


Figure 3. Comparison of the quantum yields at λ_{irr} 302.4 (full points) and 365.5 nm (open points): *trans*-AIP pressure 0.25 ± 0.02 Torr; (\bullet, \circ) = $\Phi_{t \rightarrow d}$; ($\blacktriangle, \triangle$) = $\Phi_{t \rightarrow t}$.

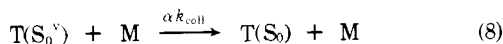
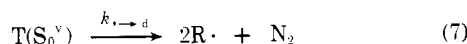
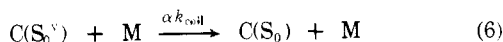
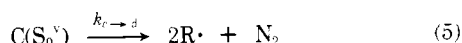
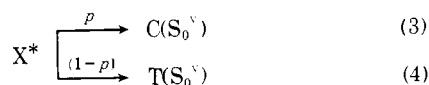
Table II. Quantum Yields of Azoisopropane Photoreactions in Solution^a

Starting isomer	Solvent	$\Phi_{t \rightarrow c}$	$\Phi_{c \rightarrow t}$	$\Phi_{t \rightarrow d}$	$\Phi_{c \rightarrow d}$
Trans	Water	0.50 ± 0.04	0.54 ± 0.04	0	
		0.38 ± 0.03^b	0.49 ± 0.03^b	0	
	Isooctane	0.53 ± 0.04	0.46 ± 0.04	0.021	
Cis	Water	0.56 ± 0.03	0.48 ± 0.03^b		0
	Isooctane	0.51 ± 0.04	0.54 ± 0.04		0.02

^a λ_{irr} 365.5 nm, temp $25 \pm 2^\circ C$. ^bReference 15. ^cReference 29.

occurs at lower pressures, independent of starting isomer and wavelength, than does the buildup of *cis*-AIP. For example, the data in Figures 1 and 2 show that $\Phi_{t \rightarrow t}$ and $\Phi_{c \rightarrow t}$ have come up to their limiting values at about 400 Torr of added CO₂, while $\Phi_{t \rightarrow c}$ and $\Phi_{c \rightarrow c}$ are still quite low at that pressure. (2) In the high pressure limit and in solution, $\Phi_{t \rightarrow c} \sim \Phi_{c \rightarrow t} \sim \Phi_{t \rightarrow t} \sim \Phi_{c \rightarrow c} \sim 0.5$. These data together with the information in (1) indicate that the photolysis of both isomers proceed via common intermediate(s). (3) There is no detectable temperature dependence in solution phase photoisomerization. This implies that there cannot be significant energy barriers in the excited state(s) toward isomerization.³ (4) There are marked wavelength dependences in the gas phase; $\Phi_{t \rightarrow d}$ and $\Phi_{c \rightarrow d}$ increase while $\Phi_{t \rightarrow c}$ and $\Phi_{t \rightarrow t}$ (and $\Phi_{c \rightarrow c}$ and $\Phi_{c \rightarrow t}$) decrease with decreasing excitation wavelength (Figure 3). (5) When the reciprocals of the decomposition quantum yields given in Figures 1 and 2 are plotted against the pressure of added CO₂ as a Stern-Volmer (S-V) plot, the curves are nonlinear, flattening at high pressures. Wu and Rice³³ first observed similar curvature when hexafluoroazomethane was photolyzed at pressures ranging to 700 Torr. They suggested that two states were dissociating at different rates; these states were either two different electronic states or different configurations of the same electronic state. The curvature that has been reported in the S-V plots for hexafluoroacetone,^{34,35} which both fluoresces and phosphoresces, has been attributed to dissociation from an excited singlet and an excited triplet state. Servedio and Pritchard³⁶ have recently suggested that the curvature they detected in the S-V plot for room-temperature photolysis of *trans*-AIP at 366 nm, which was previously reported by Arin and Steel,¹⁷ similarly results from decomposition of vibrationally excited singlet (S₁^v) and triplet (T₁^v) states.

The five criteria listed above can be fulfilled by assuming that following irradiation *cis*- and *trans*-AIP reach a common configuration X*, which populates the vibrationally excited *cis* and *trans* ground states, C(S₀^v) and T(S₀^v), with almost equal probability ($p \sim 0.5$). The vibrationally excited molecules can then either decompose or be collisionally deactivated. We shall discuss later the nature of X*.



As in the case of azo-*tert*-butane,^{16,32} the activation energy for thermal decomposition, E_a , of the *cis* isomer of AIP³⁷ is less than that of the *trans* isomer.²¹ The Arrhenius parameters for *cis*-AIP thermolysis were determined as $E_a = 40.7 \pm 1.8$ kcal mol⁻¹ and $\log A = 17.5 \pm 0.9$ (s⁻¹), while those for *trans*-AIP are 47.9 ± 1.0 kcal mol⁻¹ and 16.6 (s⁻¹), respectively. The lifetime of a C(S₀^v) molecule could then be significantly shorter than that of a T(S₀^v) molecule possessing the same excess vibrational energy. C(S₀^v) would thus require higher pressures than T(S₀^v) to be deactivated and, over an extended pressure range, the S-V plots would exhibit curvature, consistent with deactivating the longer-lived T(S₀^v) at lower pressures than the shorter lived C(S₀^v). This would also explain the fact that

at all wavelengths $\Phi_{t \rightarrow t} > \Phi_{t \rightarrow c}$ (and $\Phi_{c \rightarrow t} > \Phi_{c \rightarrow c}$) at a given pressure.

As is common in unimolecular theory,³⁸ it was assumed that the collisional deactivation efficiency of AIP was unity, i.e., $\alpha_{AIP} = 1$, so that for a molecular diameter of 7 \AA ,^{7,33} k_{coll} at 25° is calculated as $3.11 \times 10^{11} \text{ M}^{-1} \text{ s}^{-1}$. α_{CO_2} was found by comparing the quantum yields of pure *trans*-AIP at several concentrations (365.5 nm, room-temperature photolysis) with those measured for *trans*-AIP and added CO₂. The data in Figure 4 show that $\alpha_{CO_2} = 0.34 \pm 0.02$, in good agreement with the values for CO₂ obtained in other studies.³⁹ Some of the earlier results of Riem and Kutschke are also plotted in Figure 4 to demonstrate the good correlation between the two studies. It should be noted that some of the previous investigations of AIP photochemistry^{7,36} have employed *trans*-AM as an actinometer, assuming that for *trans*-AM $\Phi_{t \rightarrow d} = 1.0$ at pressures up to 1 atm.^{31,40} However, Westbrook⁴¹ has recently reported that $\Phi_{t \rightarrow d} > 1.0$ at *trans*-AM pressures less than 50 Torr upon irradiation at 366 nm. The earlier values of $\Phi_{t \rightarrow d}$ for *trans*-AIP would, therefore, depend upon the *trans*-AM concentration used in the actinometry.

The model presented above yields

$$\Phi_{c \rightarrow c} = \Phi_{t \rightarrow c} = p\alpha k_{coll}[M]/(k_{c \rightarrow d} + \alpha k_{coll}[M]) \quad (9)$$

$$\Phi_{t \rightarrow t} = \Phi_{c \rightarrow t} = (1-p)\alpha k_{coll}[M]/(k_{t \rightarrow d} + \alpha k_{coll}[M]) \quad (10)$$

$$\Phi_{c \rightarrow d} = \Phi_{t \rightarrow d} = (1-p)k_{t \rightarrow d}/(k_{t \rightarrow d} + \alpha k_{coll}[M]) + pk_{c \rightarrow d}/(k_{c \rightarrow d} + \alpha k_{coll}[M]) \quad (11)$$

In solution or at very high pressures where $k_{coll}[M] \gg k_{c \rightarrow d}$ and $k_{t \rightarrow d}$, $\Phi_{t \rightarrow t} = \Phi_{c \rightarrow t} = (1-p)$ and $\Phi_{c \rightarrow c} = \Phi_{t \rightarrow c} = p$. The solution data in Table II show that the above quantum yields are all ~ 0.5 . Moreover, with 1250 Torr of added CO₂, $\Phi_{t \rightarrow t} = 0.54 \pm 0.02$ on photolysis at 365.5, 334.2, and 302.4 nm. The same value was obtained for $\Phi_{c \rightarrow t}$ and $\Phi_{t \rightarrow t}$ for black-light irradiation (see Figures 1 and 2). p was therefore taken as 0.50. Since $\Phi_{c \rightarrow c} = \Phi_{t \rightarrow c}$, the proposed mechanism predicts the same pressure variation in the quantum yields of *cis* formation regardless of starting isomer, and the same should be true for *trans* formation. This is exactly what is observed, since $\Phi_{t \rightarrow t}$ and $\Phi_{c \rightarrow t}$ come up to their limiting values at much lower pressures than do $\Phi_{t \rightarrow c}$ and $\Phi_{c \rightarrow c}$, independent of which isomer is photolyzed.

Determination of Rate Constants from Experimental Data.

The above equations and the experimental variation in the quantum yields as functions of pressure allow the determination of $k_{t \rightarrow d}$ and $k_{c \rightarrow d}$ at a particular wavelength. Interestingly, these rate constants are most readily obtained using the isomerization and return to starting material quantum yields, since the decomposition yields contain both $k_{t \rightarrow d}$ and $k_{c \rightarrow d}$ as unknowns (see eq 11). Employing eq 9 and 10, where $\alpha k_{coll}[M]$ was replaced by $(k_{coll}[AIP] + \alpha_{CO_2}k_{coll}[CO_2])$, $k_{t \rightarrow d}$ and $k_{c \rightarrow d}$ were varied to determine calculated dependences of the former quantum yields on added CO₂ pressure that best matched the experimental results. This procedure is illustrated in Figure 5 for the extraction of $k_{t \rightarrow d}$ at 365.5 nm. The data obtained by this curve-fitting technique are listed in Table III.

A simple diagram summarizing the pertinent energies in the model is given in Figure 6. Examining the data in Table III, it can be seen that the same values are found for $k_{t \rightarrow d}$ and $k_{c \rightarrow d}$ regardless of which isomer is photolyzed when the difference in the heats of formation of the ground-state molecules, ~ 8 kcal mol⁻¹,^{32,42} is taken into account. The higher ground-state energy for *cis* acyclic azoalkanes in general relative to the corresponding *trans* isomer is reflected in the greater thermal lability of the former^{3,16,32} and in the ease with which they undergo tautomerization to the related hydrazone.^{3,31} The rate constants determined from photolyzing *cis*-AIP at 365.5 and 334.2 nm are thus approximately the same as those obtained

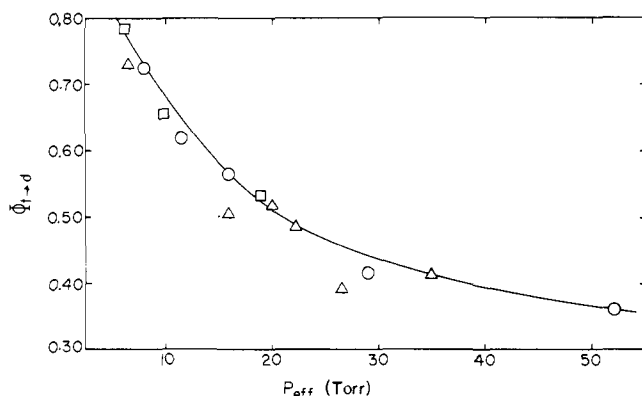


Figure 4. Pressure dependence of decomposition quantum yields for *trans*-azoisopropane, where $P_{\text{eff}} = P_{\text{trans-AIP}} + 0.34 P_{\text{CO}_2}$ and $\lambda_{\text{irr}} 365.5$ nm; (O) *trans*-AIP pressure 0.25 ± 0.02 Torr, varying CO_2 pressure; (□) pure *trans*-AIP; (Δ) data from ref 7, pure *trans*-AIP.

Table III. Rate Constants for the Decomposition of Vibrationally Excited *cis*- and *trans*-Azoisopropane at Various Excitation Wavelengths^a

Irradiation wavelength, nm	Photon energy, kcal einstein ⁻¹	$10^{-8} k_{t \rightarrow d}$, s ⁻¹	$10^{-9} k_{c \rightarrow d}$, s ⁻¹
365.5	78.2	1.1	2.4
355 (black light)	80.5	1.5	3.6
334.2	85.6	1.9	20.8
312.9	91.4	4.9	
302.4	94.5	10.1	
367.5 (black light)	77.8	1.9	9.7
365.5	78.2	1.7	3.7
334.2	85.6	5.1	

^aRate constants in the first five rows obtained starting with *trans*-AIP and using values of $\Phi_{t \rightarrow t}$ and $\Phi_{t \rightarrow c}$; last three entries using *cis*-AIP and values of $\Phi_{c \rightarrow c}$ and $\Phi_{c \rightarrow t}$.

from the photolysis of *trans*-AIP at 334.2 and 312.9 nm, respectively. This is as predicted by the proposed model, since a $\text{C}(\text{S}_0^v)$ molecule formed by photolyzing *trans*-AIP with light of energy $E_\lambda(T)$ is the same as a $\text{C}(\text{S}_0^v)$ molecule formed by the photolysis of *cis*-AIP with light of energy $E_\lambda(C)$.

Calculation of Rate Constants. The absolute values expected for $k_{t \rightarrow d}$ and $k_{c \rightarrow d}$ can be readily estimated from RRKM theory^{43,44} using the methods largely pioneered by Rabinovitch and co-workers.⁴⁵ The specific rate constant for a molecule with total energy E is given to a good approximation by

$$k(E) = A \left(\frac{E - E_0 + a^+ E_z^+}{E + a E_z} \right)^{s-1} \quad (12)$$

E represents the sum of E_λ , the excitation energy, and E_v , the vibrational energy associated with the ground-state molecules; s is the number of vibrational degrees of freedom, while A and E_0 are equated with the high-pressure frequency factor and activation energy in the corresponding thermal reaction. E_z^+ and E_z are the zero-point energies ($= \sum_{i=0}^s h\nu/2$) of the activated complex and reactant molecule, respectively; a^+ and a are factors which make the vibrational energy level densities equal to the exact values, as calculated by computer analysis. Formulas for determining these factors, which are weak functions of energy and which depend on the vibrational frequencies, have been detailed elsewhere.^{43,45} Typically, a varied from 0.846 to 0.861 as E was varied from 81.4 to 99.4 kcal mol⁻¹, while over the same range a^+ changed from 0.781 to 0.813. The vibrational analysis of *trans*-AIP was accomplished by (1) comparison of the detailed analysis of the ir spectrum of *trans*-AM⁴⁶ with that of *trans*-AIP^{20,47} and (2) estimation of the expected frequencies using the methods

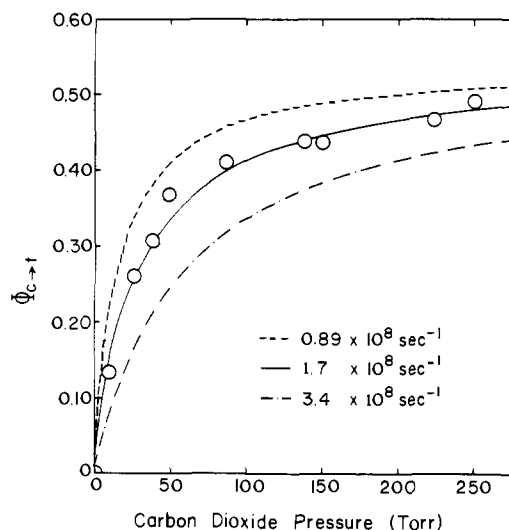


Figure 5. Determination of the decomposition rate constant, $k_{t \rightarrow d}$, for vibrationally excited *trans*-azoisopropane: $\lambda_{\text{irr}} 365.5$ nm; (O) experimental data; - - -, —, - · - model curves obtained using eq 10 for $k_{t \rightarrow d} 0.89 \times 10^8$, 1.7×10^8 , and 3.4×10^8 s⁻¹, respectively.

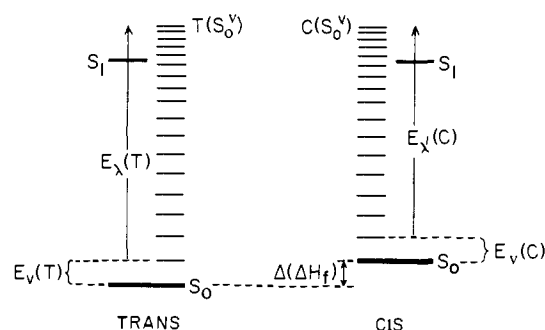


Figure 6. Energetics and states in the photochemistry of azoisopropane. $E_v(T)$ and $E_v(C)$ are the vibrational energies of the unexcited ground state molecules. $\Delta(\Delta H_f)$ is the difference in the heats of formation of the ground state (S_0) isomers. $E_\lambda(T)$ and $E_\lambda(C)$ are the excitation energies for *trans*- and *cis*-AIP to produce vibrationally excited ground state molecules, $\text{T}(\text{S}_0^v)$ and $\text{C}(\text{S}_0^v)$.

outlined by Benson.⁴⁸ A summary of the analysis is given in Table IV. Employing these data E_z was determined as 116.2 kcal mol⁻¹, in reasonable agreement with the value calculated from the vibrational analysis of *trans*-AIP assigned by Perona et al.²¹ E_z^+ , 114.5 kcal mol⁻¹, was computed by assuming that a C-N bond is breaking in the activated complex. E_v at 300 K was calculated by standard procedures⁴⁹ as 4.4 kcal mol⁻¹. It was assumed that the vibrational patterns of both isomers were similar so that $E_v(C) = E_v(T)$. The values used for A were 4.0×10^{16} and 3.2×10^{17} s⁻¹ for *trans*-²¹ and *cis*-AIP,³⁷ respectively, and for E_0 were 46.9 and 40.7 kcal mol⁻¹. In this way, $k_{t \rightarrow d}$ and $k_{c \rightarrow d}$ were calculated using only the thermal kinetic data and vibrational frequencies. The results are shown in Figures 7 and 8.

The calculated curves and the experimental points agree favorably on an absolute basis. Small changes in any of the parameters in eq 12 could make them coincident; changing any of the energy parameters (E_0 , E_z , or E_z^+) by as little as 1 kcal mol⁻¹ varies $k(E)$ by 50%. It must also be remembered that the experimental values of the decomposition rate constants are based on an estimation for k_{coll} , the deactivation rate constant of vibrationally excited *cis*- and *trans*-AIP. This quantity has an obvious uncertainty associated with it; for example, changing the collision diameter by ± 1 Å results in a $\pm 30\%$ variation in k_{coll} . The scatter in the values of $k_{t \rightarrow d}$ and $k_{c \rightarrow d}$ is probably associated with the fact that they are not

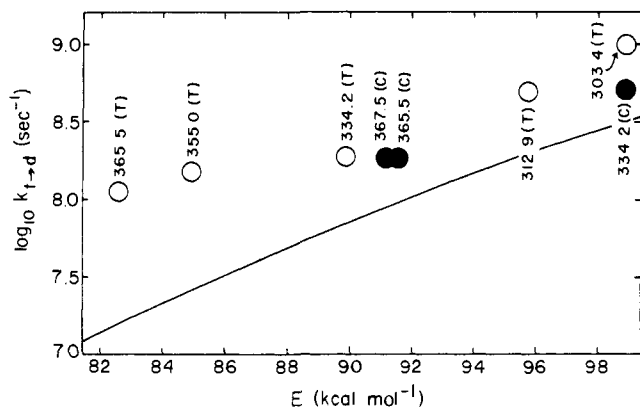


Figure 7. Rate constants for the decomposition of vibrationally excited *trans*-azoisopropane. Full line calculated from eq 12: (O) experimental values using $\Phi_{t \rightarrow t}$ and $E = E_{\lambda}(T) + E_v(T)$; (●) experimental values using $\Phi_{c \rightarrow t}$ and $E = E_{\lambda}(C) + E_v(C) + \Delta(\Delta H_f)$. Photolysis wavelength (nm) and isomer indicated beside each point.

Table IV. Vibrational Frequencies Assigned to *trans*- and *cis*-Azoisopropane in Evaluation of Rate Constants and Heat Capacities

Description of mode		No. of modes	Frequency, cm^{-1}
Stretch	N=N	1	1572
	C-N	2	1269
	C-C	4	931
	C-H	14	2912
Bend		14 (4,8,2)	1374, 1457, 1150
		4	375
		4	420
		3 (1,1,1)	312, 584, 362
Rock		8	1126
Internal rotation		4	300
		2	225

primary experimental quantities, but are determined by curve fitting techniques. In general these rate constants could only be determined to $\pm 15\%$. In Figure 9, $\Phi_{t \rightarrow d}$ at 260 ± 5 Torr of added CO_2 , a primary quantum yield, is displayed as a function of energy and compared with the curve computed using eq 11 and the calculated values of $k_{t \rightarrow d}$ and $k_{c \rightarrow d}$. The scatter is now significantly smaller.

Effects of Temperature. The proposed model predicts that temperature should affect the quantum yields since E_v is a function of temperature,⁴⁹ i.e., increasing the temperature results in the production of $T(S_0^v)$ and $C(S_0^v)$ molecules possessing larger amounts of vibrational energy and hence greater probabilities of decomposition. Vibrational heat capacities were calculated^{48,49} using the frequencies in Table IV and the temperature dependence of E_v determined. For example, in going from 27 to 172°, it was computed that E_v varied from 4.4 to 10.4 kcal mol^{-1} .

The quantum yields of the *trans*-AIP photoreactions were measured at several elevated temperatures. These quantities were corrected for the thermal decomposition of the photo-

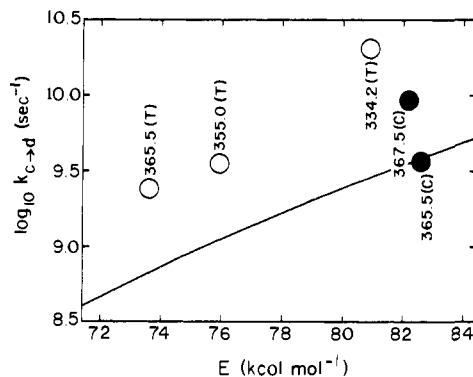


Figure 8. Rate constants for the decomposition of vibrationally excited *cis*-azoisopropane. Full line calculated from eq 12: (O) experimental values using $\Phi_{t \rightarrow c}$ and $E = E_{\lambda}(T) + E_v(T) - \Delta(\Delta H_f)$; (●) experimental values using $\Phi_{c \rightarrow c}$ and $E = E_{\lambda}(C) + E_v(C)$. Photolysis wavelength (nm) and isomer indicated beside each point.

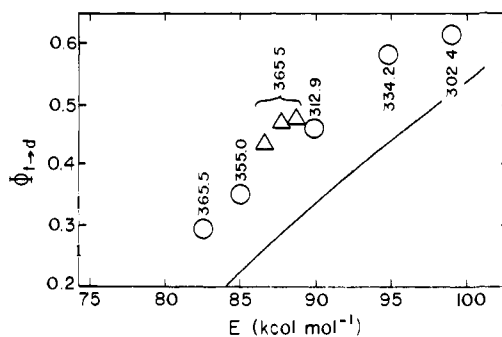


Figure 9. Decomposition quantum yield with 260 ± 5 Torr of added CO_2 (*trans*-AIP pressure 0.25 ± 0.02 Torr) as a function of energy. $E = E_{\lambda} + E_v$, where E_{λ} is the excitation energy and E_v is the vibrational energy associated with ground state *trans*-AIP. Full line calculated from eq 11 and values of $k_{c \rightarrow d}$ and $k_{t \rightarrow d}$ computed from eq 12: (O) experimental values at 299 K and wavelengths (nm) indicated; (Δ) experimental values at 403, 424, and 445 K (increasing yields) using 365.5 nm irradiation.

chemically formed *cis* isomer. Dark controls run on *trans*-AIP indicated that it did not thermolyze at these temperatures. As shown in Figure 9, the predicted and observed variations are in good agreement. It should be noted that previous studies of the effect of temperature,^{7,36} where $\Phi_{t \rightarrow d}$ was measured in terms of nitrogen formation, did not consider the pyrolysis of the *cis* isomer. This is important particularly at higher pressures, where $\Phi_{t \rightarrow c}$ becomes appreciable. For example, at 260 Torr of added CO_2 , the experimental value of $\Phi_{t \rightarrow d}$ at 172° was 0.60; when corrected for *cis*-AIP thermolysis under our conditions, it decreased to 0.48.

Sensitized Photolyses. (a) Gas Phase. The quantum yields obtained on triplet-sensitized isomerization and decomposition (${}^T\Phi_{t \rightarrow c}$ and ${}^T\Phi_{t \rightarrow d}$, respectively) of *trans*-AIP are listed in Table V. The low values are in good agreement with those previously determined for *trans*-AIP^{26,36,50} and for most other acyclic azoalkanes.^{8,9,26} The main exception is acetone- d_6 sensitization of *trans*-AM,⁸ where the decomposition yield varied from 0.29 to 0.52 as the pressure decreased from 203 to 13 Torr. In addition, there was no effect on increasing the temperature to 133°. In contrast, the acetone-sensitized decomposition of *trans*-azoisobutane at 146° occurs effectively, while at lower temperatures (112°) biacetyl was ineffective.⁹ Thus, the gas phase values of ${}^T\Phi_{t \rightarrow d}$ for the higher azoalkanes are generally less than 0.15 in the temperature region studied and the limited data indicate that ${}^T\Phi_{t \rightarrow c}$ is even smaller.

(b) Solution. The major triplet-sensitized reaction of *trans*-AIP in solution is isomerization. The values reported in Table V for this work are the initial yields, since it was found that

Table V. Triplet-Sensitized Quantum Yields for Acyclic Azoalkanes

Azo ^a (Torr or M × 10 ³)	Donor ^b (Torr or M × 10 ³)	Solvent ^c	λ _{irr} , nm	Temp, °C	TΦ _{dec} ^d	TΦ _{isom} ^d	Ref
(a) Gas Phase							
<i>trans</i> -AIP (0.173) (0.091) (0.096) (19.6) (29.8)	PhCHO (0.173)		280	25	0.12		50
	PhH (1.08)		250	25	0.09		This work
	PhH (1.07)		250	78	0.12	<0.01	This work
	(CH ₃ CO) ₂ (26.5)		436	27	0.08		26
	(CH ₃ CO) ₂		436	27, 120	V. small		36
(29.8)	(CH ₃ CO) ₂ (29.8) ^e		436	160	0.16		36
<i>trans</i> -AM (0.40) (5.45) (1.1)	(CD ₃) ₂ CO (12.4)		313	30	0.52		8
	(CD ₃) ₂ CO (149)		313	30	0.31		8
	(CD ₃) ₂ CO (202)		313	133	0.29		8
<i>trans</i> -AE (2.0)	(CD ₃) ₂ CO (66.0)		313	129	0.08		8
<i>trans</i> -ANP (16)	(CH ₃ CO) ₂ (26.0)		436	27	0.06		26
<i>trans</i> -AIB	(CH ₃) ₂ CO		313	146	0.35		9
	(CH ₃ CO) ₂		436	112	10 ⁻⁴		9
(b) Solution							
<i>trans</i> -AIP (20) (20) (7) (20) (20)	PhCOCH ₃ (13)	CH	303	25	<0.001 ^f	0.07 ± 0.02	This work
	PhCOCH ₃ (0.6)	CH	250	25	<0.001 ^f	0.07 ± 0.02	This work
	Ph ₂ CO (50)	AN	303	25		0.04 ± 0.01	This work
	PhH	M	250	22	V. small	0.04	15
	Ph ₂ CO	M	303	22	V. small	0.06	15
<i>cis</i> -AIP (7) (7)	Ph ₂ CO (50)	IO	303	25		0.70 ± 0.04	This work
	Ph ₂ CO (50)	AN	303	25		0.70 ± 0.04	This work
<i>trans</i> -AM (20) (10)	Ph ₂ CO (200)	H	366	20	0.009 ^g	>0.4	51
	PhCOCH ₃ (0.6)	IO	250	25	<0.001 ^f	0.11 ± 0.02	This work
<i>trans</i> -ATB (20.4) (10.6)	PhCOCH ₃ (51.5)	H	313	20	0.012 ^g		51
	Ph ₂ CO (50)	H	313	20	0.013 ^g		51

^a AM, AE, ANP, AIB, ATB refer to azomethane, azoethane, azo-*n*-propane, azoisobutane, and azo-*tert*-butane, respectively. Gas pressures are in Torr and solution concentrations in M × 10³. ^b Triplet energies of donors (kcal mol⁻¹): benzene (84.7); acetone (77.0); acetophenone (73.6); benzaldehyde (72.1); biacetyl (54.9). ^c CH, AN, M, IO, H refer to cyclohexane, acetonitrile, methanol, isooctane, and hexane, respectively. ^d TΦ_{dec} = TΦ_{t→d} or TΦ_{c→d} depending on starting isomer. Similarly, TΦ_{isom} = TΦ_{t→c} or TΦ_{c→t}. ^e Same value obtained with 179 Torr of added *n*-butane. ^f Determined from the absence of any detectable C₃ and C₆ hydrocarbons on VPC analysis. ^g Not corrected for simultaneous direct photolysis.

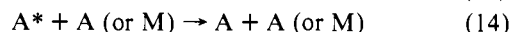
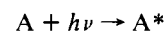
TΦ_{t→c} decreased with increased periods of photolysis as a result of the sensitized isomerization of the photochemically formed *cis* isomer back to *trans*. The low yields agree well with those previously reported¹⁵ and are much smaller than the values obtained on direct photolysis (Table II) and on singlet sensitization. However, Engel and Bartlett⁵¹ found TΦ_{t→c} = 0.4 for *trans*-AM on benzophenone sensitization at 366 nm. In the present investigation, TΦ_{t→c} for acetophenone sensitization at 250 nm, where the absorbance of *trans*-AM is a minimum, was determined as 0.11, indicating that direct photolysis could have been occurring in the previous study. In contrast to the low values of TΦ_{t→c} for *trans*-AIP, triplet-sensitized isomerization of the *cis* isomer (TΦ_{c→t}) is quite effective. Moreover, both TΦ_{t→c} and TΦ_{c→t} seem to be independent of solvent. The results show that in solution TΦ_{c→t}/TΦ_{t→c} ~ 15, while for direct photolysis Φ_{c→t}/Φ_{t→c} ~ 1. This strongly suggests that isomerization on direct photolysis does not proceed via the triplet manifold.

It is interesting to observe that the values of TΦ_{t→d} in the gas phase appear to be insensitive to the donor used and also are approximately equal to TΦ_{t→c} in solution. This may indicate that in the gas phase the triplet state lives long enough to be vibrationally relaxed so that intersystem crossing to the ground states occurs at the same energy independent of the donor and that the *cis* molecules initially formed still have enough excess energy to dissociate.

It should also be pointed out that the low triplet-sensitized yields for *trans*-AIP are not due to inefficient energy transfer. The quenching of triplet benzaldehyde in the gas phase by *trans*-AIP has been shown to occur⁵³ at a rate close to collision-controlled ($k_q = 4 \times 10^{10} \text{ M}^{-1} \text{ s}^{-1}$). In acetonitrile, triplet acetophenone is quenched by *cis*- and *trans*-AIP with $k_q = 7.5 \times 10^9$ and $3.1 \times 10^9 \text{ M}^{-1} \text{ s}^{-1}$, respectively,²⁴ while triplet benzophenone has $k_q = 4.9 \times 10^9$ and $3.8 \times 10^9 \text{ M}^{-1} \text{ s}^{-1}$.^{24,54} Knowing the triplet lifetimes (τ_{trip}) of these sensitizers under

the experimental conditions employed,^{23,53} it was ensured that $k_q[\text{Azo}] > \tau_{\text{trip}}^{-1}$. In the case of benzene, where phosphorescence emission cannot be observed, it was previously established²⁹ that the concentrations of azo used in this study effectively scavenged the triplet, but were too low to intercept singlet benzene.

Comparison with Previous Models. As mentioned in the introduction, previous studies of the gas phase photochemistry of acyclic azoalkanes have been concerned simply with the decomposition of the *trans* isomer. The pressure dependence of the nitrogen yield, Φ_{t→d} in the present nomenclature, has commonly been interpreted in terms of an excited molecule mechanism,^{6,7,25a,55-58} i.e., excitation followed by either decomposition or collisional deactivation,



This scheme leads to a S-V type equation, $1/\Phi_{t \rightarrow d} = 1 + (k_{14}[A]/k_{13})$, and over limited pressure ranges the published data did obey such an expression. Although not usually explicitly stated, it was generally assumed that A* represented the vibrationally excited ¹(*n*,π*) state reached on direct absorption, S₁^v. Pritchard et al.⁵⁷ claimed directly that the photodissociation of perfluoroazoethane occurs from this state. After treating the photodecomposition of azoethane by classical unimolecular theory (RRK), Worsham and Rice⁵⁸ concluded that S₀^v was not the decomposing state. Bowers⁵⁹ later carried our further calculations based on their data and fitted them to a model in which S₁ was the dissociative state.

However, Calvert and co-workers⁹ excluded S₁ as the dissociative state for azoisobutane, since the natural radiative lifetime (τ_{rad}) of this state, as computed from the integrated absorption spectrum, and the observed lifetime of the de-

composing state ($1/k_{13}$) predicted a quantum yield of fluorescence $> 10^{-3}$, while no emission could be detected. They suggested instead that decomposition occurred from the upper vibrational levels of the $^3(n, \pi^*)$ state, T_1^v , and isomerization from the lower levels. Abram et al.¹⁵ used similar reasoning to exclude S_1 as the dissociative state for *trans*-AIP. To explain the inefficient isomerization of *trans*-AIP on triplet sensitization (population of T_1) in solution, they suggested that this state was probably not involved in direct photolysis. Decomposition could occur instead from the upper vibrational levels of the $^3(\pi, \pi^*)$ state, T_2^v . By analogy with ethylene, the $^3(\pi, \pi^*)$ state might have an equilibrium geometry corresponding to 90° rotation about the N-N bond and so would be common for both *cis*- and *trans*-AIP. On deactivation, this state would yield ground state isomers with equal probability, a situation that was observed in solution.

Recent evidence indicates that their arguments were incorrect. An electron impact study of *trans*-AM⁶⁰ suggests that $^3(\pi, \pi^*)$ lies above $^1(n, \pi^*)$, so that intersystem crossing from the latter to the former would be energetically unfavorable. Moreover, SCF-MO calculations on diimide,⁶¹ N_2H_2 , show that as rotation is carried out about the N-N bond, the energy of $^3(\pi, \pi^*)$ increases and that it is the $^3(n, \pi^*)$ state which has an energy minimum at a geometry intermediate between those of the ground state isomers. Since the $^3(n, \pi^*)$ surface crossed the ground state surface, Baird and Swenson,⁶¹ therefore, suggested that $^3(n, \pi^*)$ was involved in the isomerization of azoalkanes. However, as pointed out in the last section, this is not in agreement with the experimental facts, since the triplet sensitization results for both the *cis* and *trans* isomers are so different from those obtained on direct photolysis.

As discussed earlier, any model that considers only one dissociative state cannot explain the curvatures observed in S-V plots over sufficiently wide pressure ranges. To interpret their nitrogen yields for the direct photolysis of *trans*-AIP, Servedio and Pritchard³⁶ suggested that decomposition arose from both S_1^v and T_1^v , while deactivation of the latter resulted in isomerization. Thus, on collisional deactivation, the *cis* and *trans* isomers should build up at the same rates. In fact, the present quantum yields show that the *trans* isomer is formed at lower pressures than the *cis*, independent of starting isomer or wavelength. Moreover, the data indicate that the shorter-lived state on deactivation yields *cis*-AIP, while the longer lived results in *trans*-AIP. The model proposed by Servedio and Pritchard would therefore require S_1 and T_1 to be common to both isomers and yet on deactivation, these states would have to yield exclusively *cis*- and *trans*-AIP, respectively. Moreover, on triplet sensitization mass balance requires $^T\Phi_{t \rightarrow d} + ^T\Phi_{t \rightarrow c} + ^T\Phi_{t \rightarrow i} = 1.0$. However, the above model predicts $^T\Phi_{t \rightarrow c} \sim ^T\Phi_{t \rightarrow i}$, so that at high pressures or in solution where deactivation ensures $^T\Phi_{t \rightarrow d} \sim 0$, $^T\Phi_{t \rightarrow c} \sim 0.5$. Again, this is inconsistent with the experimental results.

We have recently carried out calculations⁶² using the new SCF-MO method of Halgren and Lipscomb,⁶³ which is based on partial retention of diatomic differential overlap. The results for diimide agree pleasingly with those of Vasudevan et al.⁶⁴ and of Baird and Swenson.⁶¹ For azomethane, as for diimide, there is no energy barrier for rotation in the $^1(n, \pi^*)$ and $^3(n, \pi^*)$ states, but the former state now touches the ground state surface when the angle of rotation is close to 90° . The important point is that there is apparently a route for rapid internal conversion to the *cis* and *trans* ground states which does not involve the triplet manifold and has no energy barriers, so that X^* can be identified with the common $^1(n, \pi^*)$ state. The $^3(n, \pi^*)$ state also crosses the ground-state surface, but the former is now sufficiently low in energy so that there are two well-separated intersection points with the ground state surface. There is thus no a priori reason why the isomerization yields obtained by direct and triplet-sensitized photolyses

should be the same. These MO calculations and their implications in azoalkane photochemistry will be discussed fully in a later paper.

Conclusions

In the proposed mechanism, the thermal kinetics, thermochemistry, and photochemistry of AIP have been combined into a self-consistent model in which a common $^1(n, \pi^*)$ state reached on excitation undergoes rapid internal conversion to the upper vibrational levels of the *cis* and *trans* ground states. From these states there is either decomposition or collisional deactivation. Excitation to a state from which there is no barrier to rotation and from which there is very rapid internal conversion would also offer an explanation for the structureless nature of the $n \rightarrow \pi^*$ absorption band³ and the lack of any observed fluorescence and phosphorescence.⁶⁻¹¹ Strong evidence that the dissociation occurs from the same two states in the photolysis of both isomers is the identity of their photochemistries when allowance is made for the difference in their heats of formation. The model correctly predicts that the observed curvature in the S-V plots for both $\Phi_{t \rightarrow d}$ and $\Phi_{c \rightarrow d}$ over wide pressure ranges and shows why it is only at high pressures that $\Phi_{t \rightarrow i}$ equals $\Phi_{t \rightarrow c}$ and $\Phi_{c \rightarrow c}$ equals $\Phi_{c \rightarrow i}$.

The absolute lifetimes of the two dissociative states as functions of excitation energy and temperature are adequately accounted for by RRKM theory, where the Arrhenius parameters for the thermal decompositions of the isomers are employed. Some of the earlier unimolecular calculations were certainly inadequate in that they generally used classical RRK theory^{11,58} and more importantly, omitted to take into consideration the possible presence of the *cis* isomer.^{17,59}

It is attractive to speculate that the photochemistry of other acyclic azoalkanes can be accounted for with the same model proposed for AIP. However, detailed calculations cannot be performed since, with the exception of azo-*tert*-butane,^{16,32} the thermal parameters for the other *cis* azoalkanes are as yet unknown and the detailed photochemistries of both isomers for other compounds are also unavailable.

Acknowledgment. The authors gratefully acknowledge the experimental assistance of Elliot Androphy and Abraham M. Rennert and the financial support of the National Science Foundation through Grants GP-18808 and GP-35980-X.

References and Notes

- (1) Abstracted from Ph.D. Thesis of L. D. Fogel, Brandeis University, Waltham, Mass., 1974.
- (2) Author to whom inquiries should be sent.
- (3) P. S. Engel and C. Steel, *Acc. Chem. Res.*, **6**, 275 (1973).
- (4) O. P. Strausz, J. W. Lown, and H. E. Gunning, "Comprehensive Chemical Kinetics", Vol. 5, C. H. Bamford and C. F. H. Tipper, Ed., Elsevier, New York, N.Y., 1972, pp 566-696.
- (5) T. Koenig, "Free Radicals", Vol. 1, J. K. Kochi, Ed., Wiley, New York, N.Y., 1973, pp 113-155.
- (6) H. Cerfontain and K. O. Kutschke, *Can. J. Chem.*, **36**, 344 (1958).
- (7) R. H. Riem and K. O. Kutschke, *Can. J. Chem.*, **38**, 2332 (1960).
- (8) R. E. Rebbert and P. Ausloos, *J. Am. Chem. Soc.*, **87**, 1847 (1965).
- (9) S. S. Collier, D. H. Slatyer, and J. G. Calvert, *Photochem. Photobiol.*, **7**, 737 (1968).
- (10) D. H. Slatyer, S. S. Collier, and J. G. Calvert, *J. Am. Chem. Soc.*, **90**, 268 (1968).
- (11) B. S. Solomon, T. F. Thomas, and C. Steel, *J. Am. Chem. Soc.*, **90**, 2249 (1968).
- (12) C. H. Chang, R. F. Porter, and S. H. Bauer, *J. Am. Chem. Soc.*, **92**, 5313 (1970).
- (13) R. Renaud and L. C. Leitch, *Can. J. Chem.*, **32**, 545 (1954).
- (14) R. Ohme, H. Preuschhof, and H. U. Heyne, *Org. Synth.*, **52**, 11 (1972).
- (15) I. I. Abram, G. S. Milne, B. S. Solomon, and C. Steel, *J. Am. Chem. Soc.*, **91**, 1220 (1969).
- (16) T. Mill and R. S. Stringham, *Tetrahedron Lett.*, 1853 (1969).
- (17) M. L. Arin and C. Steel, *J. Phys. Chem.*, **76**, 1685 (1972).
- (18) C. G. Hatchard and C. A. Parker, *Proc. R. Soc. London, Ser. A*, **235**, 518 (1956).
- (19) J. G. Calvert and J. N. Pitts, Jr., "Photochemistry", Wiley, New York, N.Y., 1967, p 783.
- (20) L. D. Fogel, Ph.D. Thesis, Brandeis University, Waltham, Mass., 1974.
- (21) M. J. Perona, P. C. Beadle, and D. M. Golden, *Int. J. Chem. Kinet.*, **5**, 495 (1973).
- (22) S. Malkin and E. Fischer, *J. Phys. Chem.*, **68**, 1153 (1964).

- (23) L. Giering, M. Berger, and C. Steel, *J. Am. Chem. Soc.*, **96**, 953 (1974).
 (24) L. Giering, Ph.D. Thesis, Brandeis University, Waltham, Mass., 1974.
 (25) (a) J. O. Terry and J. H. Futrell, *Can. J. Chem.*, **45**, 2327 (1967); (b) C. A. Heller and A. S. Gordon, *J. Phys. Chem.*, **62**, 709 (1958); (c) J. C. J. Thynne, *Trans. Faraday Soc.*, **58**, 1392 (1962).
 (26) S. Yamashita, K. Okumura, and T. Hayakawa, *Bull. Chem. Soc. Jpn.*, **46**, 2744 (1973).
 (27) R. W. Durham and E. W. R. Steacie, *Can. J. Chem.*, **31**, 377 (1953).
 (28) S. Toby and J. Nimoy, *J. Phys. Chem.*, **70**, 867 (1966).
 (29) W. D. K. Clark and C. Steel, *J. Am. Chem. Soc.*, **93**, 6347 (1971).
 (30) (a) P. S. Dixon, A. P. Stefani, and M. Szwarc, *J. Am. Chem. Soc.*, **85**, 2551 (1963); (b) M. Matsuoka, P. S. Dixon, A. P. Stefani, and M. Szwarc, *Proc. R. Soc., London*, **314** (1962).
 (31) R. F. Hutton and C. Steel, *J. Am. Chem. Soc.*, **86**, 745 (1964).
 (32) P. S. Engel and D. J. Bishop, *J. Am. Chem. Soc.*, **97**, 6754 (1975).
 (33) E. E. Wu and O. K. Rice, *J. Phys. Chem.*, **72**, 542 (1968).
 (34) (a) P. G. Bowers and G. P. Porter, *J. Phys. Chem.*, **70**, 1622 (1966); (b) D. A. Whytock and K. O. Kutschke, *Proc. R. Soc., London, Ser. A*, **306**, 503, 541 (1968).
 (35) F. M. Servedio and G. O. Pritchard, *Int. J. Chem. Kinet.*, **7**, 195 (1975).
 (36) F. M. Servedio and G. O. Pritchard, *Int. J. Chem. Kinet.*, **7**, 99 (1975).
 (37) L. D. Fogel, A. M. Rennert, and C. Steel, *J. Chem. Soc., Chem. Commun.*, 537 (1975).
 (38) H. S. Johnston, "Gas Phase Reaction Rate Theory", Ronald Press, New York, N.Y., 1966, pp 101-103, 141.
 (39) (a) S. C. Chan, B. S. Rabinovitch, J. T. Bryant, L. D. Spicer, T. Fujimoto, Y. N. Lin, and S. P. Pavlou, *J. Phys. Chem.*, **74**, 3160 (1970); (b) R. Atkinson and B. A. Thrush, *Proc. R. Soc., London, Ser. A*, **316**, 123, 131, 143 (1970); (c) S. W. Orchard and B. A. Thrush, *ibid.*, **337**, 143 (1974); (d) S. H. Luu and J. Troe, *Ber. Bunsenges. Phys. Chem.*, **77**, 325 (1973).
 (40) (a) G. R. Hoey and K. O. Kutschke, *Can. J. Chem.*, **37**, 769 (1959); (b) M. H. Jones and E. W. R. Steacie, *J. Chem. Phys.*, **21**, 1018 (1953).
 (41) C. W. Westbrook, Ph.D. Thesis, University of North Carolina at Chapel Hill, 1973.
 (42) P. S. Engel, J. L. Wood, J. A. Sweet, and J. L. Margrave, *J. Am. Chem. Soc.*, **96**, 2381 (1974).
 (43) P. J. Robinson and K. A. Holbrook, "Unimolecular Reactions", Wiley, New York, N.Y., 1972.
 (44) (a) K. J. Laidler, "Theories of Chemical Reaction Rates", McGraw-Hill, New York, N.Y., 1969, p 160 ff; (b) B. S. Rabinovitch and D. W. Setser, *Adv. Photochem.*, **3**, 1 (1964).
 (45) (a) D. W. Setser and B. S. Rabinovitch, *Can. J. Chem.*, **40**, 1425 (1962); (b) G. Z. Whitten and B. S. Rabinovitch, *J. Chem. Phys.*, **38**, 2466 (1963).
 (46) J. R. Durig, C. B. Pate, and W. C. Harris, *J. Chem. Phys.*, **56**, 5652 (1972).
 (47) R. J. LeFevre, M. F. O'Dwyer, and R. L. Weiner, *Aust. J. Chem.*, **14**, 317 (1961).
 (48) S. W. Benson, "Thermochemical Kinetics", Wiley, New York, N.Y., 1968, p 23 ff.
 (49) (a) J. Kestin and J. R. Dorfman, "A Course in Statistical Thermodynamics", Academic Press, New York, N.Y., 1971, p 259; (b) O. K. Rice, "Statistical Mechanics, Thermodynamics, and Kinetics", W. H. Freeman, San Francisco, Calif., 1967, p 46.
 (50) I. L. Goldblatt, Ph.D. Thesis, Brandeis University, Waltham, Mass., 1972.
 (51) P. S. Engel and P. D. Bartlett, *J. Am. Chem. Soc.*, **92**, 5883 (1970).
 (52) (a) C. C. Wamser, *J. Am. Chem. Soc.*, **95**, 2044 (1973); (b) C. C. Wamser, R. T. Medary, I. E. Kochevar, N. J. Turro, and P. L. Chang, *ibid.*, **97**, 4864 (1975).
 (53) M. Berger, I. L. Goldblatt, and C. Steel, *J. Am. Chem. Soc.*, **95**, 1717 (1973).
 (54) (a) W. D. K. Clark, A. D. Litt, and C. Steel, *J. Am. Chem. Soc.*, **91**, 5413 (1969); (b) W. D. K. Clark, A. D. Litt, and C. Steel, *Chem. Commun.*, 1087 (1968).
 (55) R. W. Durham and E. W. R. Steacie, *Can. J. Chem.*, **31**, 377 (1953).
 (56) J. R. Dacey, W. C. Kent, and G. O. Pritchard, *Can. J. Chem.*, **44**, 969 (1966).
 (57) G. O. Pritchard, W. A. Mattinen, and J. R. Dacey, *Int. J. Chem. Kinet.*, **2**, 191 (1970).
 (58) W. C. Worsham and O. K. Rice, *J. Chem. Phys.*, **46**, 2021 (1967).
 (59) P. G. Bowers, *J. Phys. Chem.*, **74**, 952 (1970).
 (60) O. A. Mosher, M. S. Foster, W. M. Flicker, J. L. Beauchamp, and A. Kuppermann, *J. Chem. Phys.*, **62**, 3424 (1975).
 (61) N. C. Baird and J. R. Swenson, *Can. J. Chem.*, **51**, 3097 (1973).
 (62) N. Camp, I. R. Epstein, and C. Steel, unpublished results.
 (63) T. A. Halgren and W. M. Lipscomb, *J. Chem. Phys.*, **58**, 1569 (1973).
 (64) K. Vasudevan, S. D. Peyerimhoff, R. J. Buenker, W. E. Kammer, and H. Hsu, *Chem. Phys.*, **7**, 187 (1975).

Thermolyses of *tert*-Butyl $\Delta^{1,1'}$ -Dicyclohexenylperoxyacetate. Electrocyclic and Other Transformations of a Pentadienyl Radical

Roland E. Lehr,* J. Michael Wilson, John W. Harder, and Patrick T. Cohenour

Contribution from the Department of Chemistry, Oklahoma University, Norman, Oklahoma 73069. Received May 30, 1975

Abstract: Pentadienyl radical precursor, *tert*-butyl $\Delta^{1,1'}$ -dicyclohexenylperoxyacetate (**1**), has been synthesized and the products of its thermolysis have been determined at a variety of temperatures. Ambient temperature vacuum thermolysis affords noncyclized trienes and noncyclized *tert*-butyl ethers by disproportionation and recombination of the radical pair, respectively. An almost twofold preference for recombination at the central carbon atom of the pentadienyl system was observed. At 210 °C, thermolysis affords three additional major products, methylated dienes that arise from recombination of the pentadienyl radical with methyl radical. At 210 °C and above, an additional product, a cyclized diene (**9a**) is formed. Its stereochemistry corresponds to that which would result from conrotatory electrocyclic closure of the pentadienyl radical to a cyclopentenyl radical, followed by disproportionation. The presence of the corresponding diene **9b** that would result from disrotatory closure of the pentadienyl radical could not be conclusively established. If present, it accounts for no more than 13% of the cyclized diene mixture. At higher temperatures, products arising from hydrogen abstraction and methyl recombination of the cyclopentenyl radical are observed. Only those products with anti-backbone (conrotatory closure) were observed (by GLC comparison with authentic samples). These results point to at least a highly stereoselective cyclization of the pentadienyl radical and establish that the HOMO of the pentadienyl radical is not the factor controlling the stereochemical course of the cyclization.

Two little-explored properties of the pentadienyl radical are the regiochemistry of its recombination with other radicals and the stereochemistry of its cyclization. The latter property is particularly interesting because of conflicting theoretical predictions of the simple MO methods, which vary from stereospecific disrotatory cyclization (HOMO symmetry control)¹ to possible nonstereospecificity (state correlation diagrams² and the PMO method³). Further, more sophisticated calculations^{4,5} for the related cyclopropyl radical \rightarrow allyl radical reaction yield a stereochemical prediction opposite that based upon the HOMO method.

We chose to generate pentadienyl radical (**2**) by thermolysis of perester **1**. The anticipated transformations by which it was hoped to answer the above questions are indicated in Scheme I.

Results and Discussion

Synthesis and Properties of *tert*-Butyl $\Delta^{1,1'}$ -Dicyclohexenylperoxyacetate (1**).** The pentadienyl radical precursor was synthesized by the sequence of reactions indicated in Scheme II. The perester was obtained as a white solid, mp 34–35 °C. It could be stored under nitrogen in a freezer at –20 °C for